

# PLORA: EFFICIENT LORA HYPERPARAMETER TUNING FOR LARGE LANGUAGE MODELS

## Anonymous authors

Paper under double-blind review

## ABSTRACT

Low-rank Adaptation (LoRA) has gained popularity as a fine-tuning approach for Large Language Models (LLMs) due to its low resource requirements and good performance. While a plethora of work has investigated improving LoRA serving efficiency by serving multiple LoRAs concurrently, existing methods assume that a wide range of LoRA adapters are available for serving. In our work, we conduct extensive empirical studies to identify that current LoRA training paradigms do not utilize hardware resources efficiently and require high overhead to obtain a performant LoRA adapter. Leveraging these insights, we propose PLORA, which automatically orchestrates concurrent LoRA fine-tuning jobs under given hardware and model constraints and develops performant kernels to improve training efficiency. Our experimental studies show that PLORA reduces the makespan of LoRA fine-tuning over a given hyperparameter search space by up to  $7.52\times$  and improves training throughput by up to  $12.8\times$  across a range of state-of-the-art LLMs.

## 1 INTRODUCTION

Large Language Models (LLMs) have become the backbone of numerous modern AI applications, spanning natural language understanding, code generation, multimodal reasoning, and specialized domains such as healthcare and finance Guo et al. (2025); Grattafiori et al. (2024); Yang et al. (2024). The paradigm of pre-training followed by fine-tuning has enabled models to achieve state-of-the-art performance when adapted to specific tasks Ouyang et al. (2022).

However, fine-tuning large models for multiple tasks or user-specific applications poses a significant challenge due to the high computational cost of training and serving numerous fine-tuned variants. To address this, parameter-efficient fine-tuning (PEFT) techniques such as Low-Rank Adaptation (LoRA) [Hu et al. \(2021a\)](#) have emerged as scalable alternatives to full fine-tuning. LoRA significantly reduces the number of trainable parameters by introducing low-rank decomposition matrices into Transformer layers, allowing for specialization while keeping the pre-trained model weights frozen. This versatile deployment approach has become popular, and several systems have been recently developed to serve multiple LoRA adapters concurrently [Sheng et al. \(2023\)](#); [Chen et al. \(2024\)](#).

Existing LoRA-related inference systems, such as vLLM Kwon et al. (2023), SLoRA Sheng et al. (2023), and LoRAX Zhao et al. (2024), operate under the assumption that LoRA adapters are already well-trained and a LoRA checkpoint with decent model quality is available for a given downstream task. In this paper, we focus on the question of *how to train such LoRA adapters efficiently*.

Similar to other deep learning methods, we find that the effectiveness of LoRA fine-tuning hinges on selecting appropriate hyperparameters (§2.2). In the context of LoRA, hyperparameter tuning extends beyond standard parameters, such as learning rate and batch size. LoRA-specific parameters that need to be tuned include: 1. LoRA rank, which controls the dimensionality of the adapter matrices. A higher rank increases the expressive power but comes at a higher memory and computation cost Hu et al. (2021a). 2. A scaling factor  $\alpha$ , which determines the impact of the LoRA adapters on the pre-trained weights. We conduct a large-scale empirical study and demonstrate that there is no single rule of thumb for tuning LoRA hyperparameters. Through more than 1,000 experiments, we demonstrate that different tasks (e.g., mrpc Wang et al. (2018) or gsm8k Cobbe et al. (2021)) require different hyperparameter configurations to achieve optimal performance on various base models, highlighting the need for LoRA hyperparameter tuning.

054 However, traditional hyperparameter tuning techniques Kandasamy et al. (2020); Bergstra and  
 055 Bengio (2012); Bergstra et al. (2011) only focus on reducing the number of tuning runs and do not  
 056 account for the unique characteristics of LoRA adapters, leading to significant inefficiencies. Unlike  
 057 conventional fine-tuning, where each configuration is trained in isolation, we aim to enable *multiple*  
 058 *LoRA adapters to be trained concurrently within the same run*. We refer to this setting as **intra-run**  
 059 training. Since LoRA adapters are **heterogeneous** and have **varying resource requirements** (§2.3),  
 060 intra-run settings open up new optimization opportunities. For example, we find that many LoRA  
 061 configurations evaluated during hyperparameter tuning have small batch sizes and underutilize GPU  
 062 hardware resources, with SM occupancy around 16.7% and memory utilization less than 55%. Based  
 063 on these observations, we propose *packing multiple LoRA configurations* during hyperparameter  
 064 tuning, thereby sharing hardware resources across configurations and improving utilization.

065 We develop PLORA, an automated concurrent LoRA training system. Given a base model and a  
 066 predefined hyperparameter search space, PLORA orchestrates efficient LoRA fine-tuning jobs and  
 067 executes them with packed LoRA adapters. PLORA operates in two stages: an offline planning  
 068 stage followed by an online execution stage. We first design an offline packing planner that analyzes  
 069 the hyperparameter search space and creates jobs with packed LoRA configurations that maximize  
 070 throughput. The planner also determines the appropriate degree of parallelism for each job. We  
 071 formulate the planner as an optimization problem and design an efficient approximate algorithm with  
 072 provable performance bounds (§5).

073 In the second stage, the jobs created by the planner are deployed by an online LoRA Execution  
 074 Engine. The execution engine monitors available hardware resources and launches multiple tuning  
 075 jobs concurrently if sufficient resources are available. We also design new GPU kernels for packed  
 076 LoRA adapters that are used once a job is launched, and show that our kernels can achieve near-linear  
 077 speedups for up to 32 adapters across various base models. In summary, we make the following  
 078 contributions:

- 079 • We conduct a large-scale empirical study with more than 1,000 experiments to demonstrate  
 080 the necessity of optimizing LoRA hyperparameters.
- 081 • We develop an algorithm to automatically allocate multiple LoRA fine-tuning tasks to jobs  
 082 while accounting for hardware, model, and LoRA configuration constraints.
- 083 • We demonstrate that PLORA reduces the total hyperparameter tuning makespan by up to  
 084 7.52× when tuning more than 100 configurations.

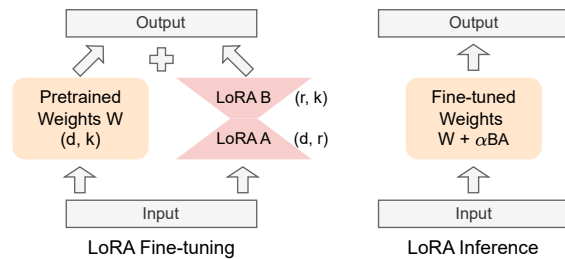
## 085 2 HYPERPARAMETER TUNING IN LORA

### 086 2.1 LOW-RANK ADAPTATION (LORA)

088 Low-Rank Adaptation (LoRA) Hu et al. (2021a) is a widely adopted efficient fine-tuning technique  
 089 for Large Language Models (LLMs). Formally, for a weight matrix  $W \in \mathbb{R}^{d \times k}$ , LoRA adds the  
 090 weight updates  $\Delta W$  as two small matrices  $A \in \mathbb{R}^{d \times r}$  and  $B \in \mathbb{R}^{r \times k}$ , where  $r$  is the LoRA rank and  
 091 much smaller than  $d$  and  $k$ . The additional FLOPs incurred by LoRA is linear to its rank. LoRA  
 092 only updates  $A$  and  $B$ , thus significantly reducing computation and storage costs for fine-tuning.  
 093 During inference, LoRA merges the multiplied matrix  $\Delta W = B \times A$  into the original  
 094 weight matrix  $W$  with a scaling factor  
 095 LoRA alpha  $\alpha$  and the weight matrix becomes  
 096  $W = W + \alpha \Delta W$ , as shown in Figure 1.

### 097 2.2 HYPERPARAMETER SPACE

101 Hyperparameter tuning is a fundamental process in developing deep learning models, involving  
 102 selecting optimal values for parameters not learned during training Bergstra et al.  
 103 (2011). These hyperparameters include, but  
 104 are not limited to, the *learning rate*, which determines the step size for updating model weights,  
 105 and the *batch size*, which defines the number of samples processed before a weight update. LoRA  
 106 fine-tuning also requires hyperparameter tuning and introduces additional hyperparameters, such



107 Figure 1: This figure demonstrates how LoRA is applied to weight matrices in fine-tuning and inference.

108  
109  
110  
111  
112  
113  
114  
115  
116  
117  
118  
119  
120  
121  
122  
123  
124  
125  
126  
127  
128  
129  
130  
131  
132  
133  
134  
135  
136  
137  
138  
139  
140  
141  
142  
143  
144  
145  
146  
147  
148  
149  
150  
151  
152  
153  
154  
155  
156  
157  
158  
159  
160  
161

Table 1: Hyperparameters for LoRA fine-tuning. LoRA alpha is a scaling factor on LoRA updates.

Hyperparameters	Search range
Learning rate (LR)	2e-5 ~ 4e-4
Batch size (BS)	1 ~ 32
LoRA rank (r)	8 ~ 128
LoRA alpha ( $\alpha$ )	$r/4 \sim 4r$

Table 3: This table analyzes LoRA hyperparameter sensitivity. The base model is QWen-2.5-7B. We only tune one hyperparameter and keep the others fixed. The results are the maximum accuracy differences by tuning the chosen hyperparameter.

Task	LR	BS	Rank	$\alpha$
mrpc	8.5%	10.0%	6.4%	4.9%
cola	14.2%	8.5%	13.1%	5.9%
wnli	6.8%	11.3%	5.4%	5.5%
gsm8k	5.0%	3.2%	4.5%	2.5%

Table 2: This table shows the optimal hyperparameter configuration we found during the hyperparameter sweep.

Task	3B				7B			
	Rank	LR	BS	$\alpha$	Rank	LR	BS	$\alpha$
mrpc	16	4e-5	1	1	32	6e-5	1	1
cola	64	4e-4	1	0.25	32	8e-5	1	0.5
wnli	32	2e-4	2	1	32	2e-4	4	0.5
gsm8k	32	1e-4	2	1	16	3e-4	1	1

Table 4: Model quality of QWen-2.5-7B with the base model only, the worst, and the best LoRA hyperparameter configuration across various tasks.  $\Delta$  represents the accuracy improvements between the best configuration and the base model.

	Base	Worst	Best	$\Delta$
mrpc	64.1%	57.1%	70.0%	+5.9%
cola	62.7%	61.5%	80.2%	+18.5%
wnli	78.8%	74.7%	84.5%	+5.7%
gsm8k	70.8%	71.2%	79.8%	+9.0%

as *LoRA rank* and *LoRA alpha*, which are specifically related to LoRA adapters. The set of hyperparameters studied in this paper for LoRA fine-tuning is listed in Table 1. Introducing these LoRA-specific hyperparameters expands the search space of hyperparameter tuning, making the process more complex and challenging.

### 2.3 STUDY OF LORA HYPERPARAMETER TUNING

We perform an extensive empirical study of the impact of hyperparameters on model quality with LoRA fine-tuning. The detailed experimental setup is described in §6. We use QWen-2.5 Yang et al. (2024) as the base model and report the zero-shot accuracy on the following benchmarks in our experiments: **GSM8K** Cobbe et al. (2021) for mathematical reasoning; **mrpc** Wang et al. (2018) for language understanding; **cola** Wang et al. (2018) for commonsense reasoning; and **wnli** Wang et al. (2018) for logic reasoning.

**Observation #1: Hyperparameters strongly influence LoRA model quality.** We investigate both individual and collective impacts of hyperparameters on model quality. First, by varying only one hyperparameter at a time (Table 3) while fixing others to the optimal configuration in Table 2, we find accuracy differences of up to 14.2% (learning rate), 11.3% (batch size), 13.1% (LoRA rank), and 5.9% (LoRA  $\alpha$ ). Second, by evaluating 120 LoRA configurations (Table 4) built from the search space in Table 1, we observe that hyperparameters collectively have a substantial effect: while some configurations degrade accuracy below that of the pre-trained base model (e.g., **wnli** drops from 78.8% to 74.7%), careful tuning can yield significant improvements (e.g., **cola** +18.5%, **wnli** +5.7%, **gsm8k** +9.0%).

We also study how the best LoRA configurations vary across different LoRA fine-tuning workloads, which are evaluated using both QWen-2.5-3B and QWen-2.5-7B as base models. The best LoRA configurations for different workloads are listed in Table 2.

**Observation #2: Optimal LoRA configurations vary across tasks and base models.** Table 2 shows that the best hyperparameter settings for LoRA fine-tuning depend on both the downstream task and the base model. For instance, with QWen-2.5-3B, the best configuration for **mrpc** is [16, 4e-5, 1, 1], while **gsm8k** requires [32, 1e-4, 2, 1]; applying the **mrpc** configuration to **gsm8k** reduces accuracy by 7.4%. Similarly, transferring the best configuration for **cola** on QWen-2.5-7B to QWen-2.5-3B decreases accuracy by 3.6%. These results highlight that effective LoRA fine-tuning requires workload- and model-specific configurations.

162 **Observation #3: LoRA fine-tuning benefits from small batch sizes.** As shown in Table 2, LoRA  
 163 consistently achieves higher accuracy with smaller batch sizes ( $\leq 4$ ), a trend also reported in  
 164 prior work Zhao et al. (2024); Hu et al. (2021a); Fomenko et al. (2024). Smaller batches reduce  
 165 gradient variance when only a fraction of parameters are updated, which improves convergence and  
 166 generalization Hu et al. (2021a).

### 168 3 EFFICIENT LORA HYPERPARAMETER TUNING

170 Next, we investigate the system efficiency of LoRA fine-tuning. We first discuss systems challenges  
 171 in searching for the best LoRA configuration in a large search space. We then propose a new LoRA  
 172 fine-tuning paradigm that significantly optimizes throughput for LoRA hyperparameter tuning, and  
 173 discuss some new systems challenges that arise.

#### 175 3.1 HARDWARE UNDERUTILIZATION

176 **SM underutilization.** We profile the SM occupancy for single LoRA fine-tuning on an A100 GPU  
 177 with QWen-2.5-7B on Unslloth Daniel Han and team (2023). While we vary batch size from 1 to  
 178 16 and rank from 8 to 128, the SM occupancy remains constant at 16.7% for both base model and  
 179 LoRA kernels. This constant low occupancy arises because LoRA’s much smaller matrices lack the  
 180 arithmetic intensity and shared memory data reuse needed to fully utilize the tensor cores, suggesting  
 181 that most SM resources sit idle during adapter updates.

182 **Memory underutilization.** When a single LoRA configuration is fine-tuned for a given set of  
 183 hardware resources, GPU memory is often also underutilized. This underutilization arises from two  
 184 factors: 1) The base model remains frozen, so only the relatively small LoRA adapter is updated, and  
 185 2) LoRA fine-tuning typically uses small batch sizes, further reducing memory demand.

186 **Existing hyperparameter tuning approaches fall short.** Existing hyperparameter tuning techniques,  
 187 such as grid search Bergstra et al. (2011), and Bayesian optimization Kandasamy et al. (2020), focus  
 188 on reducing the number of tuning runs and are agnostic to the time taken or resources required  
 189 for each configuration. Thus, when applying these approaches to LoRA fine-tuning, the hardware  
 190 resource is still underutilized during each LoRA configuration run.

#### 192 3.2 OUR PROPOSAL: LORA FINE-TUNING WITH PACKED LORA CONFIGURATIONS

194 To address the above challenges, we propose  
 195 packing multiple LoRA configurations for sim-  
 196 taneous fine-tuning, thereby sharing the same  
 197 hardware resources to improve hardware utili-  
 198 zation.

199 **Packing LoRA adapters is feasible.** Each  
 200 LoRA configuration corresponds to a distinct  
 201 LoRA adapter, while the base model remains  
 202 identical across all configurations, as its weights  
 203 are frozen during LoRA fine-tuning. This in-  
 204 sight motivates the idea of packing multiple  
 205 LoRA configurations into a single fine-tuning  
 206 job, thereby avoiding out-of-memory (OOM)  
 207 issues. When performing tensor parallel (or  
 208 FSDP-based Zhao et al. (2023)) distributed fine-tuning, the combined memory capacity increases,  
 209 allowing more LoRA adapters to be packed into a single fine-tuning job.

210 **Packed LoRA fine-tuning workflow.** In LoRA fine-tuning with a single LoRA adapter Hu et al.  
 211 (2021a), a single input is passed to both the base model and the LoRA adapter, and their outputs  
 212 are merged with a scaling factor  $\alpha$  for the final output, as shown in Figure 1. In contrast, packed  
 213 LoRA fine-tuning takes an array of multiple inputs with an input for each LoRA adapter, as shown in  
 214 Figure 2. All inputs are passed to the base model and their corresponding LoRA adapters. The outputs  
 215 from the base model and LoRA adapters are then merged. The computation of each adapter in packed  
 216 LoRA fine-tuning is identical to that of LoRA fine-tuning with a single LoRA adapter. Meanwhile, the  
 217 base model is shared among LoRA adapters, offering opportunities for higher hardware utilization.

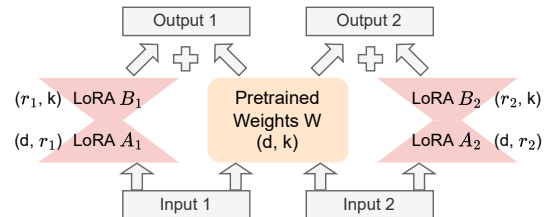


Figure 2: This figure demonstrates how PLoRA works with two LoRA adapters packed in a fine-tuning job.

216

## 3.3 CHALLENGES

217

218 Packing multiple LoRA adapters into a single fine-tuning job is analogous to increasing the batch  
 219 size, improving hardware utilization and LoRA hyperparameter tuning efficiency, but introducing  
 220 new challenges.

221

222 **Efficient computation of packed LoRA adapters on GPUs.** A packed LoRA fine-tuning job  
 223 consists of a shared base model and multiple LoRA adapters. While the base model processes the  
 224 combined input from all adapters, each adapter has distinct inputs and weights, preventing direct  
 225 merging. Naively iterating over adapters, as in Figure 2, leads to low hardware utilization in both  
 forward and backward passes due to small LoRA ranks and low arithmetic intensity.

226

**Resource-aware packed LoRA scheduling.**

227

228 Even with optimized kernels, packing adapters  
 229 efficiently is challenging because hardware can-  
 230 not hold all configurations from a large hyper-  
 231 parameter search space. We must maximize utili-  
 232 zation while avoiding OOM errors and allocate  
 233 GPU resources across fine-tuning jobs. Maxi-  
 234 mizing throughput requires jointly optimizing  
 235 both adapter packing and compute allocation;  
 236 optimizing either in isolation is insufficient.

237

**4 SYSTEM OVERVIEW OF PLORA**

238

239 We propose PLORA, a system for efficient  
 240 LoRA hyperparameter tuning via packed fine-  
 241 tuning. Given a base model, hardware pool, and  
 242 configuration search space, PLORA maximizes  
 243 tuning throughput by packing LoRA configura-  
 244 tions to fully utilize hardware resources. Fig-  
 245 ure 3 illustrates PLORA, which has two main  
 246 components: 1) a *LoRA Execution Engine* that  
 247 launches fine-tuning jobs with optimized Packed LoRA Kernels (§C), and 2) a *LoRA Packing*  
 248 *Planner* that schedules configurations by jointly  
 249 optimizing packing and hardware allocation (§5).

250

251 PLORA operates in two phases: *offline configura-  
 252 tion planning* and *online execution*. A *fine-tuning  
 253 job* is defined as fine-tuning multiple packed LoRA adapters on a shared base model. In the offline  
 254 phase, the Packing Planner explores packed configura-  
 255 tions using a cost model that estimates memory  
 256 usage and throughput from the first few iterations (10 in our testbed). The Job Planner then deter-  
 257 mines packing strategies, allocates hardware resources, and enqueues planned jobs.

258

259 In the online phase, the Execution Engine dynami-  
 260 cally dequeues jobs based on available hardware.  
 261 Its Job Launcher sets up parallelism strategies and deploys packed jobs, while the Resource Monitor  
 262 tracks resource availability. PLORA can run multiple jobs concurrently as long as resources suffice.  
 263 Customized Packed LoRA Kernels improve GPU utilization during both forward and backward  
 264 propagation (Appendix C).

265

266 Upon job completion, each adapter is stored in the Checkpoint Pool, and the released hardware  
 267 resources are returned to the pool. The Resource Monitor then triggers execution of the next queued  
 268 jobs, ensuring continuous and efficient hardware use.

269

**5 SCHEDULING OF PACKED LORA FINE-TUNING**

270

271 This section describes how to schedule packed LoRA configurations for LoRA hyperparameter tuning.  
 272 We first formalize the optimization problem by jointly considering LoRA configuration packing  
 273 and hardware allocation for fine-tuning jobs. Since the formulation is NP-complete, we develop an  
 274 approximate algorithm for this problem and analyze its performance.

275

276 The optimization goal is to minimize the *makespan* of training time for all configurations in the given  
 277 search space on the specified hardware. We observe that the completion time of a LoRA fine-tuning  
 278 job is mainly affected by two factors: **1. The packed LoRA configurations**, which determine the set

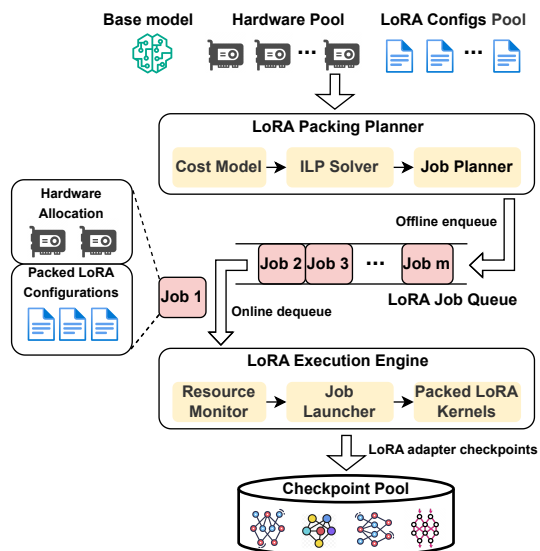


Figure 3: The system architecture of PLORA.

270 of LoRA adapters fine-tuned in a job. **2. The degree of parallelism**, which determines the number of  
271 GPUs used for each fine-tuning job.  
272

273 The optimization problem aims to minimize the  
274 makespan  $t_{opt}$ . The detailed formulation can be  
275 found in Appendix A. This optimization prob-  
276 lem is NP-complete as it can be viewed as a  
277 variant of a 0-1 knapsack problem Karp (2009).  
278 Our goal is to solve the makespan problem  
279 (Eq. 8). We approximate this by maximizing in-  
280 stantaneous throughput (Eq. 1), which we solve  
281 with DTM (Alg. 1) and prove is near-optimal  
282 (Appendix D). In addition, our optimization  
283 formulation adds a new layer of complexity, as  
284 each job must first decide which LoRA con-  
285 figurations ( $\mathcal{H}_{jk}$ ) to train and determine the  
286 associated degree of parallelism.

287 Since the LoRA FLOP (floating-point operations of adapters, excluding the base model) is fixed  
288 given a hyperparameter search space, minimizing the makespan ( $t_{opt}$ ) is equivalent to maximizing the  
289 average LoRA FLOP over this time. Thus, the optimization problem can be rewritten in throughput  
290 form as  $\max \frac{\sum_{k=1}^{|K|} FLOP_k}{t_{opt}}$ , where  $FLOP_k$  denotes the FLOP of configuration  $k$ . Because solving  
291 this problem exactly is intractable, we next develop an approximation algorithm to address it.  
292

293 Computing an optimal job schedule for average  
294 throughput is challenging, so we instead maxi-  
295 mize *instantaneous throughput* at the job level.  
296 This leads to a scheduling algorithm with prov-  
297 able bounds relative to the optimal solution.  
298

### 299 **Maximizing fine-tuning job throughput.**

300 Given  $G$  GPUs and a set of LoRA configura-  
301 tions  $K$ , we approximate minimizing makespan by maximizing throughput (Expression 1).  
302

303 Note that we use LoRA rank in Eq (1) instead  
304 of LoRA FLOP by leveraging the linear scaling  
305 property of LoRA FLOP in rank (refer to §2.1).  
306 Here  $r_k$  is the rank of configuration  $k$ ,  $m$  the  
307 number of concurrent jobs,  $d_j$  the parallelism  
308 degree of job  $j$ ,  $M_{\text{base}}$  the base model memory,  
309  $M_{\text{lora},k}$  the LoRA memory,  $M_{\text{gpu}}$  the GPU capac-  
310 ity, and  $C \in (0, 1]$  a load factor. Constraints 2–5  
311 enforce memory, GPU, and parameter ranges.  
312

313 **ILP Solvable with determined parallelism de-  
314 gree.** We note that the problem is nonconvex  
315 because  $T(\mathcal{H}_{j,k}, d_j)$  depends on  $d_j$ . However,  
316 since  $d_j$  takes power-of-two values, we can enu-  
317 merate the denominator. We thus solve a re-  
318 stricted ILP where parallelism is fixed at  $D \leq G$ .  
319 Here  $\mathcal{H}_k$  indicates whether configuration  $k$  is  
320 selected. We solve  $F(D, K)$  recursively with  
321 a DTM algorithm (Alg. 1): for each  $D$ , the  
322 solver optimizes  $F(D, K)$ , then recursively ap-  
323 plies ILP to the remaining subproblems. The  
324 recursion terminates when no GPUs remain or  
325 all configurations are scheduled. Among all can-  
326 didate schedules  $P$ , the one with the minimum  
327 makespan is selected.  
328

$$\max \sum_{j=1}^m \frac{\sum_{k=1}^{|K|} \mathcal{H}_{j,k} * r_k}{T(\mathcal{H}_{j,k}, d_j)}, \quad (1)$$

$$\text{s.t. } M_{\text{base}} + \sum_{k=1}^{|K|} \mathcal{H}_{j,k} * M_{\text{lora},k} \leq C * M_{\text{gpu}} * d_j, \quad (2)$$

$$\forall 1 \leq j \leq m$$

$$\Sigma_j d_j \leq G, \quad 1 \leq j \leq m \quad (3)$$

$$1 \leq d_j \leq G, \quad d_j \in \{2^i \mid i \in \mathbb{N}\} \quad (4)$$

$$m \geq 1, \quad m \in \mathbb{Z} \quad (5)$$

$$F(D, K) = \frac{\sum_{k=1}^{|K|} \mathcal{H}_k * r_k}{T(\mathcal{H}_k, D)}, \quad (6)$$

$$\text{s.t. } M_{\text{base}} + \sum_{k=1}^{|K|} \mathcal{H}_k * M_{\text{lora},k} \leq C * M_{\text{gpu}} * D, \quad (7)$$

**Algorithm 1:** Decomposed Throughput Maxi-  
mization (DTM)

**Input:** Number of GPUs  $G$ , LoRA configura-  
tion space  $K$

**Output:** Scheduling policy, which is a set of  
packed LoRA configurations and their  
parallelism degrees.

---

```

1 def DTMHelper( $g, P_{\text{tmp}}, K, P$ ) :
2   if  $g \leq 0$  or  $K = \emptyset$  then
3      $P \leftarrow P \cup P_{\text{tmp}}$  ;
4     return ;
5    $g' \leftarrow 2^{\lfloor \log_2 g \rfloor}$  ;           // Round down
6   //  $d$  represents parallelism
7   // degree
8   foreach  $d \in \{g', g'/2, \dots, 1\}$  do
9     // Call Gurobi ILP solver
10     $P_{\text{new}}, K_{\text{used}} \leftarrow F(d, K)$  ;
11    DTMHelper( $g - d$ ,
12                $P_{\text{tmp}} \cup P_{\text{new}}, K - K_{\text{used}}$ ) ;
13
14 def DTM( $G, K$ ) :
15    $P \leftarrow \emptyset$  ;
16   DTMHelper( $G, \emptyset, K, P$ ) ;
17   return  $\arg \min \{T(p) \mid p \in P\}$  ;

```

---

324 **The job planner.** Algorithm 1 focuses on finding the best packing of LoRA configurations on the  
 325 available GPUs to maximize concurrent throughput. It determines which configurations to train  
 326 together and to what degree of parallelism. The job scheduling algorithm then takes these packed  
 327 groups and decides the order in which they should run on the hardware, producing a complete job  
 328 queue. Together, these two algorithms first determine the most efficient packing of configurations  
 329 (Algorithm 1) and then schedule those packs over time (job scheduler) (Algorithm 2). This overall  
 330 process approximately solves Problem (1), which is equivalent to minimizing the makespan, by  
 331 ensuring that hardware is kept as fully utilized as possible throughout execution.

332 The core principle for the job planner is to schedule packed LoRA fine-tuning jobs with the maximum  
 333 concurrent throughput whenever hardware resources are available. If there are available GPU  
 334 resources for job scheduling (Line 4), it invokes  $DTM()$  introduced in Algorithm 1 to find the best  
 335 set of packed LoRA fine-tuning jobs for these available resources (Line 5) and updates the remaining  
 336 LoRA configurations (Line 7). The job planner also adds the set of jobs to the LoRA job queue (Line  
 337 8). It then predicts the next job completion event with the cost model and updates the number of  
 338 available GPUs for the next round of job planning.

339 **Computation time of the job planner.** The run-  
 340 ning time of the job planner is negligible, espe-  
 341 cially considering this is for offline scheduling.  
 342 Since solving each optimization instance takes  
 343 less than a second and all recursive branches  
 344 can be performed in parallel, we observe that  
 345 the computation time of Algorithm 1 is within  
 346 10 minutes in our evaluation with 120 config-  
 347 urations on 8 GPUs (§6.2), less than 2.5% of the  
 348 overall duration. In Appendix D, we prove the  
 349 near-optimality of the scheduling algorithm.

## 350 6 EVALUATION

351 In this section, we will demonstrate the effective-  
 352 ness of PLORA for LoRA hyperparameter tun-  
 353 ing. Specifically, we will address the following  
 354 questions: 1. Can PLORA reduce the makespan  
 355 of LoRA hyperparameter tuning? (§6.2) 2. Does  
 356 PLORA find better LoRA adapters that improve model quality? (§6.4) We also conduct detailed  
 357 ablation studies to evaluate each component’s performance.

### 358 6.1 EXPERIMENT SETUP

360 **Testbed.** We conduct experiments with a G5 and a P4d 24xlarge instance from Amazon EC2. The  
 361 P4d instance has 8 A100 GPUs (40 GB) connected by NVLink for GPU-to-GPU communication. The  
 362 G5 instance has 8 A10 GPUs (24 GB) connected by PCIe Gen4 for GPU-to-GPU communication.

363 **Models and tasks.** We conduct experiments on the Qwen 2.5 model family, one of the frontier  
 364 open-weight model families that provides the most complete model size selections, including, but not  
 365 limited to 3B, 7B, 14B, and 32B, and on LLAMA-3.2-3B and LLAMA-3.1-8B. We perform our  
 366 evaluation in a zero-shot setting, following the prompting template in prior work Zhao et al. (2024).  
 367 We use four downstream tasks, GSM8K Cobbe et al. (2021), mrpc Wang et al. (2018), cola Wang  
 368 et al. (2018), and wnli Wang et al. (2018) and set sequence length to 1024.

369 **LoRA configuration selection.** In LoRA hyperparameter tuning, the search space is specified by  
 370 users. The search space in our evaluations consists of four knobs: learning rate, batch size, LoRA rank,  
 371 and LoRA alpha. Their ranges are listed in Table 1. We select a total of 120 LoRA configurations for  
 372 the experiments.

373 **Baselines.** We compare PLORA with sequential approaches for LoRA hyperparameter tuning, in  
 374 which each LoRA fine-tuning job only evaluates one LoRA adapter. We consider two strategies for  
 375 sequential approaches: *Min GPU*, which uses the minimum set of hardware that satisfies the memory  
 376 constraints for each LoRA fine-tuning job and launches parallel jobs to fill all GPUs; and *Max GPU*,  
 377 which uses the maximum number of devices within a GPU instance for each LoRA fine-tuning job,  
 i.e., setting TP degree to 8 in our testbed. While we evaluate it with tensor parallelism, we believe the

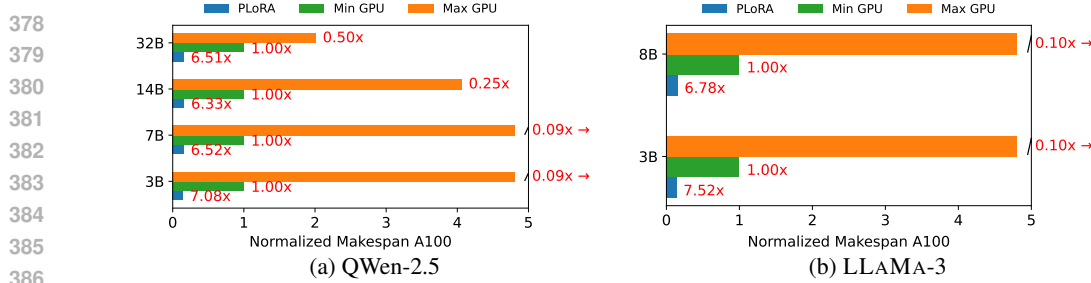


Figure 4: The makespan of LoRA hyperparameter tuning with different methods on A100 GPUs. The makespan is normalized to the performance of Min GPU.

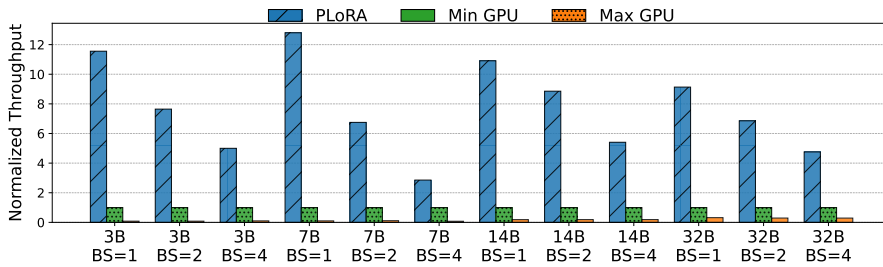


Figure 5: LoRA fine-tuning job throughput for various QWen-2.5 model sizes and batch sizes (BS) on A100 GPUs. The performance is normalized to Min GPU.

proposed design is also applicable to other parallelisms, such as pipeline parallelism Narayanan et al. (2019) and FSDP Zhao et al. (2023), which are part of our future work.

**Metrics.** We use the makespan to evaluate the end-to-end performance of LoRA hyperparameter tuning, which evaluates all LoRA configurations in the search space. We use throughput to evaluate the performance of LoRA fine-tuning jobs and packed LoRA kernels. We report the zero-shot accuracy on the downstream tasks.

**Implementation.** We implement a prototype of PLoRA atop torchtune torchtune (2024). Our implementation contains around 5000 lines of Python code and around 800 lines of code in a CUTLASS-based CUDA implementation for customized packed LoRA kernels. We use cvxpy Diamond and Boyd (2016) to implement our optimization module and built upon the PyTorch DTensor primitive to customize LoRA tensor parallel sharding strategies for efficient fine-tuning with tensor parallelism.

## 6.2 MAKESPAN EVALUATION.

We evaluate PLoRA’s makespan improvement over two baselines using 120 LoRA configurations. The base models are from the QWen-2.5 family. A single GPU can fit the 3B and 7B models, while the 14B requires two GPUs and the 32B requires four. Thus, for Min GPU, we use this TP size and start concurrent jobs to fully occupy all available GPUs. For Max GPU, we use all eight GPUs per job, allowing only one job at a time.

Figure 4a shows the makespan normalized to Min GPU. The performance of Max GPU is much worse than that of Min GPU due to even lower hardware utilization. On the contrary, PLoRA reduces the makespan by 6.51× and 6.33× on 14B and 32B, respectively, thanks to packed LoRA fine-tuning. PLoRA also achieves 7.08× and 6.52× reduction in makespan on the 3B and 7B models.

We also evaluate LLAMA-3.2-3B and LLAMA-3.1-8B and observe similar improvements in makespan. Min GPU runs each LoRA fine-tuning job with one GPU, and eight concurrent jobs are launched. Max GPU still has the worst makespan, as shown in Figure 4b. PLoRA achieves 7.52× speedups over Min GPU for LLAMA-3.2-3B and 6.78× speedup for LLAMA-3.1-8B.

## 6.3 JOB-LEVEL THROUGHPUT EVALUATION.

We study the benefits of packing by measuring the throughput of packed LoRA fine-tuning jobs compared to our baselines. We run PLoRA with different base models and batch sizes on A100 GPUs. We fix LoRA rank to be 32 and other settings of PLoRA, Min GPU, and Max GPU are the

432 Table 5: Model quality comparison of different models with no LoRA, the default, and the best LoRA  
 433 configuration. The numbers in each cell are the quality of the base model, the default configuration,  
 434 the best configuration, and the quality improvement over the default configuration.

	QWen-2.5-3B	QWen-2.5-7B	LLAMA-3.2-3B	LLAMA-3.1-8B
mrpc	62.4 / 62.6 / 67.6 <b>+5.0%</b>	64.1 / 64.7 / 70.0 <b>+5.3%</b>	70.3 / 77.4 / 80.6 <b>+3.2%</b>	71.3 / 80.3 / 84.5 <b>+4.2%</b>
cola	48.8 / 53.8 / 77.2 <b>+23.4%</b>	62.7 / 68.4 / 80.2 <b>+11.8%</b>	69.9 / 71.8 / 77.3 <b>+5.5%</b>	71.9 / 73.8 / 80.0 <b>+6.2%</b>
wnli	53.5 / 66.2 / 73.4 <b>+7.2%</b>	78.8 / 80.1 / 84.5 <b>+4.4%</b>	46.4 / 61.9 / 64.8 <b>+2.9%</b>	54.9 / 67.6 / 73.2 <b>+5.6%</b>
gsm8k	61.2 / 64.8 / 74.6 <b>+9.8%</b>	70.8 / 72.1 / 79.8 <b>+7.7%</b>	60.4 / 63.3 / 71.3 <b>+8.0%</b>	69.6 / 70.5 / 78.0 <b>+7.5%</b>

440 same as those in §6.2. We show the job throughput on QWen-2.5 models in Figure 5. We observe  
 441 similar trends in the LLAMA-3 models.

442 For a batch size of 1, PLORA achieves up to  $12.8\times$  speedup across the tested models. When we  
 443 increase the batch size, the performance gain reduces since the Min GPU strategy can better utilize  
 444 the hardware. However, the table shows that we still achieve a significant throughput improvement  
 445 for a batch size of 4. Further increasing batch sizes harms model quality, as discussed in §3.

#### 446 6.4 MODEL QUALITY WITH PLORA

447 In this section, we evaluate the model quality of the best LoRA adapter found by PLORA from the  
 448 given search space with 120 LoRA configurations. Four base models, QWen-2.5-3B, QWen-2.5-7B,  
 449 LLAMA-3.2-3B, and LLAMA-3.1-8B are fine-tuned with LoRA on four downstream tasks.

450 The model quality results are shown in Table 5. Each cell reports four numbers: (1) the base  
 451 model without LoRA, (2) the LoRA adapter fine-tuned with the default hyperparameters from  
 452 Unslooth Daniel Han and team (2023), a popular LoRA framework, (3) the best LoRA adapter found  
 453 in our search space, and (4) the quality improvement (in red) of the best configuration over the default  
 454 one. The results show that default LoRA hyperparameters already improve quality over the base  
 455 model on downstream tasks. However, they do not fully exploit LoRA’s potential. After searching  
 456 120 configurations with PLORA, the best LoRA adapters outperform the default configuration by up  
 457 to 23.4%, with consistent gains across different model families.

## 458 7 RELATED WORKS

459 **LoRA-related systems.** Efficient LoRA serving has been extensively studied. DLoRA Wu et al.  
 460 (2024), Punica Chen et al. (2024), and SLoRA Sheng et al. (2023) develop scheduling algorithms,  
 461 optimized GPU kernels, and memory management techniques for multi-LoRA serving. However,  
 462 these systems focus on LoRA serving and assume that LoRA adapters have been well-trained. A  
 463 recent work Ye et al. (2023) develops a pipeline parallel strategy for LoRA training. In contrast,  
 464 PLORA optimizes the system efficiency of LoRA hyperparameter tuning to find the best LoRA  
 465 adapter from a search space.

466 **Hyperparameter tuning.** Existing hyperparameter tuning techniques, such as grid search Bergstra  
 467 et al. (2011) and Bayesian optimization Kandasamy et al. (2020), are designed to reduce the search  
 468 space, which is orthogonal to our study. PLORA can work with different hyperparameter tuning  
 469 algorithms based on the configuration space provided to the planner. Many hyperparameter tuning  
 470 systems Dunlap et al. (2021); Mai et al. (2020); Akiba et al. (2019); Kotthoff et al. (2017); Li et al.  
 471 (2020) have also been proposed for model pretraining, however, these techniques and systems cannot  
 472 address low hardware utilization when fine-tuning a single LoRA configuration. Our work focuses on  
 473 leveraging underutilized hardware resources to sweep the hyperparameter search space.

474 **Job scheduling.** Makespan minimization is an extensively studied topic in generalized cluster job  
 475 scheduling Narayanan et al. (2020); Xiao et al. (2018); Hu et al. (2021b). These prior works on  
 476 generalized cluster scheduling assume jobs are predefined. However, in LoRA hyperparameter tuning,  
 477 PLORA’s optimization module also determines how LoRA configurations are packed into each job  
 478 and their degree of parallelism. We leverage additional information about LoRA configurations and  
 479 hardware resources to optimize job scheduling and joint allocation of GPU resources.

## 480 8 CONCLUSION

481 This paper presents PLORA, a system for efficiently tuning LoRA hyperparameters. We conduct  
 482 an extensive empirical study to demonstrate the need for LoRA hyperparameter tuning and identify  
 483 inefficiencies in current tuning pipelines. We leverage these insights to design a LoRA packing

486 planner and an execution engine and build a parallel LoRA fine-tuning framework. PLORA improves  
 487 the fine-tuning throughput by up to  $12.8\times$  over traditional approaches by packing multiple LoRA  
 488 adapters in a fine-tuning job and reduces makespan by up to  $7.52\times$  across tested models.  
 489

490 **REFERENCES**  
 491

492 Takuya Akiba, Shotaro Sano, Toshihiko Yanase, Takeru Ohta, and Masanori Koyama. 2019. Optuna:  
 493 A next-generation hyperparameter optimization framework. In *Proceedings of the 25th ACM*  
 494 *SIGKDD international conference on knowledge discovery & data mining*. 2623–2631.

495 James Bergstra, Rémi Bardenet, Yoshua Bengio, and Balázs Kégl. 2011. Algorithms for hyper-  
 496 parameter optimization. *Advances in neural information processing systems* 24 (2011).

497 James Bergstra and Yoshua Bengio. 2012. Random search for hyper-parameter optimization. *The*  
 498 *journal of machine learning research* 13, 1 (2012), 281–305.

500 Lequn Chen, Zihao Ye, Yongji Wu, Danyang Zhuo, Luis Ceze, and Arvind Krishnamurthy. 2024.  
 501 Punica: Multi-tenant lora serving. *Proceedings of Machine Learning and Systems* 6 (2024), 1–13.

502 Karl Cobbe, Vineet Kosaraju, Mohammad Bavarian, Mark Chen, Heewoo Jun, Lukasz Kaiser,  
 503 Matthias Plappert, Jerry Tworek, Jacob Hilton, Reiichiro Nakano, et al. 2021. Training verifiers to  
 504 solve math word problems. *arXiv preprint arXiv:2110.14168* (2021).

505 Michael Han Daniel Han and Unsloth team. 2023. *Unsloth*. [http://github.com/](http://github.com/unslothai/unsloth)  
 506 unslothai/unsloth

507 Tim Dettmers, Artidoro Pagnoni, Ari Holtzman, and Luke Zettlemoyer. 2023. Qlora: Efficient  
 508 finetuning of quantized llms. *Advances in neural information processing systems* 36 (2023),  
 509 10088–10115.

510 Steven Diamond and Stephen Boyd. 2016. CVXPY: A Python-embedded modeling language for  
 511 convex optimization. *Journal of Machine Learning Research* 17, 83 (2016), 1–5.

512 Lisa Dunlap, Kirthevasan Kandasamy, Ujval Misra, Richard Liaw, Michael Jordan, Ion Stoica, and  
 513 Joseph E Gonzalez. 2021. Elastic hyperparameter tuning on the cloud. In *Proceedings of the ACM*  
 514 *Symposium on Cloud Computing*. 33–46.

515 Vlad Fomenko, Han Yu, Jongho Lee, Stanley Hsieh, and Weizhu Chen. 2024. A Note on LoRA.  
 516 *arXiv preprint arXiv:2404.05086* (2024).

517 Marco Ghirardi and Chris N Potts. 2005. Makespan minimization for scheduling unrelated parallel  
 518 machines: A recovering beam search approach. *European Journal of Operational Research* 165, 2  
 519 (2005), 457–467.

520 Aaron Grattafiori, Abhimanyu Dubey, Abhinav Jauhri, Abhinav Pandey, Abhishek Kadian, Ahmad  
 521 Al-Dahle, Aiesha Letman, Akhil Mathur, Alan Schelten, Alex Vaughan, et al. 2024. The llama 3  
 522 herd of models. *arXiv preprint arXiv:2407.21783* (2024).

523 Daya Guo, Dejian Yang, Haowei Zhang, Junxiao Song, Ruoyu Zhang, Runxin Xu, Qihao Zhu,  
 524 Shirong Ma, Peiyi Wang, Xiao Bi, et al. 2025. Deepseek-r1: Incentivizing reasoning capability in  
 525 llms via reinforcement learning. *arXiv preprint arXiv:2501.12948* (2025).

526 Edward J Hu, Yelong Shen, Phillip Wallis, Zeyuan Allen-Zhu, Yuanzhi Li, Shean Wang, Lu Wang,  
 527 and Weizhu Chen. 2021a. Lora: Low-rank adaptation of large language models. *arXiv preprint*  
 528 *arXiv:2106.09685* (2021).

529 Qinghao Hu, Peng Sun, Shengen Yan, Yonggang Wen, and Tianwei Zhang. 2021b. Characterization  
 530 and prediction of deep learning workloads in large-scale gpu datacenters. In *Proceedings of the*  
 531 *International Conference for High Performance Computing, Networking, Storage and Analysis*.  
 532 1–15.

540 Kirthevasan Kandasamy, Karun Raju Vysyaraju, Willie Neiswanger, Biswajit Paria, Christopher R  
 541 Collins, Jeff Schneider, Barnabas Poczos, and Eric P Xing. 2020. Tuning hyperparameters without  
 542 grad students: Scalable and robust bayesian optimisation with dragonfly. *Journal of Machine  
 543 Learning Research* 21, 81 (2020), 1–27.

544

545 Richard M Karp. 2009. Reducibility among combinatorial problems. In *50 Years of Integer Program-  
 546 ming 1958-2008: from the Early Years to the State-of-the-Art*. Springer, 219–241.

547

548 Lars Kotthoff, Chris Thornton, Holger H Hoos, Frank Hutter, and Kevin Leyton-Brown. 2017. Auto-  
 549 WEKA 2.0: Automatic model selection and hyperparameter optimization in WEKA. *Journal of  
 550 Machine Learning Research* 18, 25 (2017), 1–5.

551

552 Woosuk Kwon, Zhuohan Li, Siyuan Zhuang, Ying Sheng, Lianmin Zheng, Cody Hao Yu, Joseph  
 553 Gonzalez, Hao Zhang, and Ion Stoica. 2023. Efficient memory management for large language  
 554 model serving with pagedattention. In *Proceedings of the 29th Symposium on Operating Systems  
 Principles*. 611–626.

555

556 Liam Li, Kevin Jamieson, Afshin Rostamizadeh, Ekaterina Gonina, Jonathan Ben-Tzur, Moritz Hardt,  
 557 Benjamin Recht, and Ameet Talwalkar. 2020. A system for massively parallel hyperparameter  
 558 tuning. *Proceedings of machine learning and systems* 2 (2020), 230–246.

559

560 Luo Mai, Guo Li, Marcel Wagenländer, Konstantinos Fertakis, Andrei-Octavian Brabete, and Peter  
 561 Pietzuch. 2020. {KungFu}: Making training in distributed machine learning adaptive. In *14th  
 562 USENIX Symposium on Operating Systems Design and Implementation (OSDI 20)*. 937–954.

563

564 Sourab Mangrulkar, Sylvain Gugger, Lysandre Debut, Younes Belkada, Sayak Paul, and Benjamin  
 565 Bossan. 2022. PEFT: State-of-the-art Parameter-Efficient Fine-Tuning methods. <https://github.com/huggingface/peft>.

566

567 Deepak Narayanan, Aaron Harlap, Amar Phanishayee, Vivek Seshadri, Nikhil R Devanur, Gregory R  
 568 Ganger, Phillip B Gibbons, and Matei Zaharia. 2019. PipeDream: Generalized pipeline parallelism  
 569 for DNN training. In *Proceedings of the 27th ACM symposium on operating systems principles*.  
 1–15.

570

571 Deepak Narayanan, Keshav Santhanam, Fiodar Kazhamiaka, Amar Phanishayee, and Matei Zaharia.  
 572 2020. {Heterogeneity-Aware} cluster scheduling policies for deep learning workloads. In *14th  
 573 USENIX Symposium on Operating Systems Design and Implementation (OSDI 20)*. 481–498.

574

575 Long Ouyang, Jeffrey Wu, Xu Jiang, Diogo Almeida, Carroll Wainwright, Pamela Mishkin, Chong  
 576 Zhang, Sandhini Agarwal, Katarina Slama, Alex Ray, et al. 2022. Training language models to  
 577 follow instructions with human feedback. *Advances in neural information processing systems* 35  
 (2022), 27730–27744.

578

579 Michael L. Pinedo. 2008. *Scheduling: Theory, Algorithms, and Systems* (3rd ed.). Springer Publishing  
 580 Company, Incorporated.

581

582 Ying Sheng, Shiyi Cao, Dacheng Li, Coleman Hooper, Nicholas Lee, Shuo Yang, Christopher Chou,  
 583 Banghua Zhu, Lianmin Zheng, Kurt Keutzer, et al. 2023. S-lora: Serving thousands of concurrent  
 584 lora adapters. *arXiv preprint arXiv:2311.03285* (2023).

585

586 Mohammad Shoeybi, Mostofa Patwary, Raul Puri, Patrick LeGresley, Jared Casper, and Bryan  
 587 Catanzaro. 2019. Megatron-lm: Training multi-billion parameter language models using model  
 588 parallelism. *arXiv preprint arXiv:1909.08053* (2019).

589

590 Vijay Thakkar, Pradeep Ramani, Cris Cecka, Aniket Shivam, Honghao Lu, Ethan Yan, Jack Kosaian,  
 591 Mark Hoemmen, Haicheng Wu, Andrew Kerr, Matt Nicely, Duane Merrill, Dustyn Blasig, Fengqi  
 592 Qiao, Piotr Majcher, Paul Springer, Markus Hohnerbach, Jin Wang, and Manish Gupta. 2023.  
 593 *CUTLASS*. <https://github.com/NVIDIA/cutlass>

594

595 torchtune. 2024. *torchtune: PyTorch's finetuning library*. <https://github.com/pytorch/torchtune>

594 Alex Wang, Amanpreet Singh, Julian Michael, Felix Hill, Omer Levy, and Samuel R Bowman. 2018.  
 595 GLUE: A multi-task benchmark and analysis platform for natural language understanding. *arXiv*  
 596 *preprint arXiv:1804.07461* (2018).

597

598 Bingyang Wu, Ruidong Zhu, Zili Zhang, Peng Sun, Xuanzhe Liu, and Xin Jin. 2024. {dLoRA}:  
 599 Dynamically orchestrating requests and adapters for {LoRA}{LLM} serving. In *18th USENIX*  
 600 *Symposium on Operating Systems Design and Implementation (OSDI 24)*. 911–927.

601

602 Wencong Xiao, Romil Bhardwaj, Ramachandran Ramjee, Muthian Sivathanu, Nipun Kwatra, Zhen-  
 603 hu Han, Pratyush Patel, Xuan Peng, Hanyu Zhao, Quanlu Zhang, et al. 2018. Gandiva: Intro-  
 604 spective cluster scheduling for deep learning. In *13th USENIX Symposium on Operating Systems*  
 605 *Design and Implementation (OSDI 18)*. 595–610.

606

607 An Yang, Baosong Yang, Beichen Zhang, Binyuan Hui, Bo Zheng, Bowen Yu, Chengyuan Li,  
 608 Dayiheng Liu, Fei Huang, Haoran Wei, et al. 2024. Qwen2. 5 technical report. *arXiv preprint*  
 609 *arXiv:2412.15115* (2024).

610

611 Zhengmao Ye, Dengchun Li, Zetao Hu, Tingfeng Lan, Jian Sha, Sicong Zhang, Lei Duan, Jie Zuo,  
 612 Hui Lu, Yuanchun Zhou, et al. 2023. mLoRA: Fine-Tuning LoRA Adapters via Highly-Efficient  
 613 Pipeline Parallelism in Multiple GPUs. *arXiv preprint arXiv:2312.02515* (2023).

614

615 Justin Zhao, Timothy Wang, Wael Abid, Geoffrey Angus, Arnav Garg, Jeffery Kinnison, Alex  
 616 Sherstinsky, Piero Molino, Travis Addair, and Devvret Rishi. 2024. LoRA Land: 310 Fine-tuned  
 617 LLMs that Rival GPT-4, A Technical Report. *arXiv preprint arXiv:2405.00732* (2024).

618

619

620

621

622

623

624

625

626

627

628

629

630

631

632

633

634

635

636

637

638

639

640

641

642

643

644

645

646

647

648 **A OPTIMIZATION FORMULATION**  
649650 The optimization problem can be formulated as follows:  
651

652 
$$\min t_{opt} \quad (8)$$
  
653

654 
$$\text{s.t. } t_{opt} \geq s_j + T(\mathcal{H}_{j,k}, d_j), \quad \forall j \in J \quad (9)$$
  
655

656 
$$\sum_{j \in J} \mathcal{H}_{jk} = 1, \quad \forall k \in K \quad (10)$$
  
657

658 
$$s_{j'} \geq s_j + T(\mathcal{H}_{j,k}, d_j) - M(1 - \mathcal{W}_{jj'}) + \mathcal{Z}_{jj'} M, \quad (11)$$
  
659

660 
$$\forall j \neq j', \quad j, j' \in J$$
  
661 
$$s_j \geq s_{j'} + T(\mathcal{H}_{j',k}, d_{j'}) - M(1 - \mathcal{W}_{jj'}) + \mathcal{Z}_{jj'} M, \quad (12)$$
  
662

663

664 
$$\forall j \neq j', \quad j, j' \in J$$
  
665

666 
$$\mathcal{Z}_{jj'} + \mathcal{Z}_{j'j} = \mathcal{W}_{jj'}, \quad \forall j \neq j', \quad j, j' \in J \quad (13)$$
  
667

668 
$$\mathcal{W}_{jj'} \leq \mathcal{X}_{ij}, \quad \mathcal{W}_{jj'} \leq \mathcal{X}_{ij'}, \quad \forall j \neq j', \quad \forall i \quad (14)$$
  
669

670 
$$\mathcal{W}_{jj'} \geq \mathcal{X}_{ij} + \mathcal{X}_{ij'} - 1, \quad \forall j \neq j', \quad \forall i \quad (15)$$
  
671

672 
$$\mathcal{X}_{ij}, \mathcal{H}_{jk} \in \{0, 1\}, \quad \forall i, \quad \forall j \in J, \quad \forall k \in K \quad (16)$$
  
673

674 
$$\mathcal{Z}_{jj'}, \mathcal{W}_{jj'} \in \{0, 1\}, \quad \forall j \neq j', \quad j, j' \in J \quad (17)$$
  
675

676 
$$s_j \geq 0, \quad \forall j \in J; \quad 1 \leq i \leq G \quad (18)$$
  
677

678 In this formulation, we input the number of hardware devices  $G$  and LoRA configurations  $K$ . The  
679 rest are variables that the optimization instances solve.  $J$  represents the set of jobs,  $\mathcal{X}_{ij}$  is a binary  
680 variable that equals 1 if job  $j$  is assigned to device  $i$ ,  $\mathcal{H}_{jk}$  is a binary parameter that indicates whether  
681 LoRA configuration  $k$  belongs to job  $j$ .  $s_j$  is the start time of job  $j$ ,  $\mathcal{Z}_{jj'}$  is a binary variable that  
682 ensures job ordering where  $\mathcal{Z}_{jj'} = 1$  if job  $j$  precedes job  $j'$  and does not overlap in time,  $\mathcal{W}_{jj'}$  is a  
683 binary variable indicating that whether job  $j$  and  $j'$  share at least one device. We employ  $M$  as an  
684 auxiliary large constant in the ordering constraints Ghirardi and Potts (2005). During optimization for  
685 minimal makespan, the optimization instance would output how LoRA configurations are assigned  
686 to jobs ( $\mathcal{H}$ ), how jobs are assigned to devices ( $\mathcal{X}$ ), and when jobs are scheduled ( $\mathcal{Z}$ ).  $T()$  is the  
687 cost model used to estimate the training time of LoRA fine-tuning jobs; it is not a variable, but a  
688 function of the packed LoRA configurations  $\mathcal{H}_{j,k}$  and the parallelism degree  $d_j$ , where  $j$  is a job.  
689 The notations used in this section are listed in Table 6.690 In our optimization setup, Equation 10 ensures that each LoRA configuration belongs  
691 to exactly one fine-tuning job; Inequalities 11, 12, and Equation 13  
692 ensure that jobs sharing any devices do not overlap in time Pinedo (2008); Inequalities 14  
693 and 15 help enforce the prior constraint by setting  $\mathcal{W}_{jj'}$  to 1 when two jobs share at least  
694 one device Pinedo (2008). The makespan is represented as the latest job completion timestamp in  
695 Inequality 9. Equations 16, 17, and 18 define the scope of  
696 the variables. This optimization problem also has constraints on GPU memory usage of each LoRA  
697 fine-tuning job and the number of GPUs that can be allocated to all concurrent jobs.698 This optimization problem is NP-complete as it can be viewed as a variant of a 0-1 knapsack  
699 problem Karp (2009). In addition, our optimization formulation adds a new layer of complexity, as  
700 each job must first decide which LoRA configurations ( $\mathcal{H}_{jk}$ ) to train and determine the associated  
701 degree of parallelism.693 **A.1 NOTATION TABLE**  
694695 Below is the notation table used in formulating the optimization problem:  
696697 **B LORA MEMORY CONSTRAINTS**  
698699 **B.1 LoRA MEMORY CONSTRAINTS**  
700701 To ensure that the training job does not exhaust the available GPU memory, we impose a constraint  
702 on the total memory used by all LoRA configurations in a job, including the base model weights. The

Table 6: Notation used in cost model formulation

Symbol	Description
<b>Model-related parameters</b>	
$C$	Memory load factor
$M_{\text{base}}$	Memory required for the base model
$M_{\text{lora},k}$	Memory required for LoRA configuration $k$
$M_{\text{gpu}}$	Total memory capacity of a GPU
$G$	Number of available GPU devices
$K$	Set of LoRA configurations
$J$	Set of training jobs
$M$	A large constant for scheduling ordering
$T()$	Duration of job, estimated with cost model
<b>Optimization variables</b>	
$\chi_{ij}$	Binary variable: 1 if job $j$ runs on device $i$
$\mathcal{H}_{jk}$	Binary variable for LoRA assignment
$s_j$	Start time of job $j$
$r_k$	LoRA rank of LoRA configuration $k$
$\mathcal{Z}_{jj'}$	Binary variable for scheduling order
$\mathcal{W}_{jj'}$	Binary variable for device sharing
$d_j$	Number of GPUs used by job $j$

total memory usage must not exceed the GPU memory:

$$M_{\text{base}} + \sum_{k=1}^K M_{\text{lora},k} \leq c_{\text{load}} \times M_{\text{gpu}}$$

$M_{\text{base}}$  represents the memory cost of the base model, while  $M_{\text{lora},k}$  represents the memory cost of a LoRA adapter on a device. Similar to other work on managing GPU memory Kwon et al. (2023), the user can set a load factor  $c_{\text{load}}$  to account for internal GPU fragmentation and adjust GPU memory usage.

For each LoRA configuration  $k$ , the memory usage,  $M_{\text{lora},k}$ , is represented by an indicator variable to determine if the user applies LoRA to those matrices. In each attention block, the user can apply LoRA to  $Q$ ,  $K$ ,  $V$ , and the output projection matrix; In each MLP block, the user can apply LoRA to the up, down, and gate projection matrix. We, therefore, write the LoRA memory usage as a sum of these 7 components:

$$M_{\text{lora},k} = \sum_{i=1}^7 \mathbb{I}_i M_{\text{lora},i} \quad (19)$$

Each index  $i$  corresponds to one of the seven components the user can apply LoRA to. For each component, the LoRA memory usage includes the memory required to store LoRA parameters, gradients, and activations:

$$M_{\text{lora},k} = M_{\text{lora.param},k} + M_{\text{lora.grad},k} + M_{\text{lora.act},k} \quad (20)$$

The memory for LoRA parameters,  $M_{\text{lora.param},k}$ , is given by:

$$M_{\text{lora.param},k} = n_{\text{layers}} (h_{\text{in}} \times r_{\text{lora},k} + h_{\text{out}} \times r_{\text{lora},k}) \times c_{\text{prec}}$$

In practice, this may change depending on memory-saving strategies such as activation checkpointing. Here,  $n_{\text{layers}}$  is the number of layers,  $h_{\text{in}}$  and  $h_{\text{out}}$  represent the input and output dimensions of the projection matrix, which can take different values based on the model architecture and vary between attention and MLP blocks.  $c_{\text{prec}}$  is the training precision, representing bytes per parameter.

The memory required for the gradients,  $M_{\text{lora.grad},k}$ , is calculated as:

$$M_{\text{lora.grad},k} = c_{\text{grad}} \times M_{\text{lora.param},k} \times c_{\text{prec}}$$

$c_{grad}$  represents the scaling factor for storing gradient-related parameters. For example, this factor is three in the popular AdamW optimizer, representing momentum, velocity, and primary gradients.

Finally, the LoRA activation memory for each block,  $M_{lora\_act,i}$ , is given by:

$$M_{lora\_act,k} = b \times s \times r_{lora,k} \times c_{prec}$$

Here  $b$  is the batch size, and  $s$  is the sequence length. This term represents the memory used to store intermediate activations during training. In LLM fine-tuning, the sequence length varies based on the workload. The standard practice is to set a maximum training length and split the training document if some data samples are too long to ensure no memory overflow. When computing memory consumption, we take the same approach and set the sequence length to the maximum length of the training samples.

Similarly, the activation memory for the base model can be computed by summing the activation of the embedding layer, the attention operator, and the feed-forward network in each layer. Depending on the implementation, other activations, such as those produced by layer norm may also be computed and stored, our model can be adapted to those implementations with ease. More details on computing the memory consumption for each of these four modules can be found in the Appendix:

$$M_{base\_act} = M_{base\_emb} + M_{base\_attn} + M_{base\_mlp}$$

The total memory for the base model is then calculated as:

$$M_{base} = M_{base\_weights} + M_{base\_act}$$

The computation in this section assumes a single-device setting. The section discusses how the parallelization strategy affects our memory constraints.

### B.1.1 PARALLELIZATION STRATEGY AND GPU CONSTRAINTS:

The prior section of constraints assumes that a full copy of the model is stored on each device. In practice, tensor parallelism, pipeline parallelism, and fully-sharded data parallelism (FSDP) are popular strategies to parallelize LLM training and are necessary for modern LLMs. The following section explains how we incorporate different parallelization strategies into our cost model. To accommodate tensor parallelism and pipeline parallelism, we can rewrite the memory cost associated with the LoRA adapters  $i$  as follows:

$$M_{lora\_param,k} = \frac{M_{lora\_param,k}}{d_{tp} * d_{pp}}$$

This is similar to base model parameters and intermediate outputs. For FSDP, the model computes the following for different levels of ZeRO optimizers. For ZeRO-1, the LoRA memory includes both the unsharded gradient and parameter memory and the sharded optimizer state:

$$M_{lora,k}^{(1)} = M_{lora\_grad,k}^{(1)} + M_{lora\_param,k} + \frac{M_{opt,k}}{d_{fsdp}}$$

For ZeRO-2, the gradient memory also includes the gradient term:

$$M_{lora,k^{(2)}} = M_{lora\_param,k} + \frac{M_{lora\_grad,k} + M_{opt,k}}{d_{fsdp}}$$

For ZeRO-3, the memory includes all fully sharded components:

$$M_{lora,k}^{(3)} = \frac{M_{lora\_param,k} + M_{lora\_grad,k} + M_{opt,k}}{d_{fsdp}}$$

Then, the model will solve for concurrent training jobs to launch and determine each job's parallelization strategy, ensuring that the total GPU usage does not exceed the GPU constraints.

We apply this formulation to every memory cost computation and add a total GPU constraint where the model will solve for the number of jobs to launch concurrently, as well as the tensor parallel degrees and LoRA adapter configurations to be packed on each job:

$$\sum_j d_j \leq G$$

810 C OPTIMIZING PACKED LoRA COMPUTATION  
811812 C.1 INEFFICIENT COMPUTATION IN EXISTING FRAMEWORKS  
813

814 LLM pre-training frameworks, such as Megatron-LM Shoeybi et al. (2019) and PyTorch Zhao  
815 et al. (2023), and LoRA fine-tuning frameworks, such as PEFT Mangrulkar et al. (2022) and  
816 Unslloth Daniel Han and team (2023), only support fine-tuning one configuration on a set of hardware  
817 at a time. Since LoRA adapters, when packed, share the same base model weights but have different  
818 adapter weights and inputs<sup>1</sup>, a naive approach to support fine-tuning with packed LoRA adapters is to  
819 batch the computation of the base model and sequentially compute each LoRA adapter (Figure 2).  
820 However, this approach results in poor fine-tuning throughput due to low hardware utilization when  
821 computing each LoRA adapter.

822 We profiled the fine-tuning performance using the naive approach as described above. We use  
823 Qwen-2.5-7B as the base model and apply a single LoRA adapter with batch size 1 on an A100 GPU  
824 as the baseline. The iteration time increases by 10% when the batch size is increased from 1 to 8.  
825 However, when we pack eight adapters into a fine-tuning job and each adapter has a batch size of  
826 1, the naive approach worsens the iteration time by  $3.6 \times$  compared to single LoRA tuning due to  
827 low hardware utilization in LoRA adapter computations. We also observe similar performance when  
828 fine-tuning Qwen-2.5-14B with two A100 GPUs and Qwen-2.5-32B with four A100 GPUs using TP.  
829 This confirms our hypothesis that the performance bottleneck is the sequential computation of LoRA  
830 adapters rather than the batched computation in the base model.

831 C.2 PACKED LoRA KERNELS  
832

833 We devise custom CUDA kernels for PLORA to efficiently batch the computation of LoRA adapters  
834 in both forward and backward propagations. We carefully tile the LoRA matrices and group gradient  
835 computations across multiple adapters to improve hardware utilization and handle load balancing for  
836 heterogeneous LoRA adapters.

837 Given a set of LoRA adapters, we concatenate the LoRA adapters into a tensor and design kernels  
838 which can compute forward and backward passes for all LoRA adapters. Our key insight in designing  
839 performant kernels is to tile the concatenated tensor along the sequence or hidden dimensions if  
840 possible. The sequence dimension consists of the input token sequence multiplied by the batch size.  
841 We avoid tiling along the LoRA rank dimension because the rank can be as small as 8, and sharding  
842 on the smaller dimension prevents GPUs from fully utilizing their compute resources.

843 If we denote the dimension of LoRA A by  $(d, r)$  and the dimension of LoRA B by  $(r, k)$  (Figure 1),  
844 we typically have  $d \gg r$  and  $r \ll k$ . Previous work on serving multiple LoRA adapters Chen et al.  
845 (2024) introduces a kernel that handles these two cases separately, by splitting the input dimension  $d$   
846 for LoRA A and the output dimension  $k$  for LoRA B. While this is possible for the forward pass,  
847 backward propagation cannot simply reuse this strategy. When computing the activation gradients  
848 with respect to LoRA inputs, avoiding tiling over the rank dimension would require splitting the  
849 inner dimension for tiling. This strategy would require extra overhead in creating a scratch buffer  
850 for each tile, additional indices for bookkeeping, and extra synchronization and reduction steps  
851 for accumulating intermediate results, which would undermine the benefits of tiling over large  
852 dimensions.

853 In our work, we tackle the challenge of efficient backward propagation implementation and use the  
854 following strategy to obtain performant kernels.

855 **CUDA kernel design.** We built upon CUTLASS for our packed LoRA kernels. Four cases should be  
856 considered separately for the upstream weights and input gradients of LoRA A and LoRA B. Below,  
857 we outline our partitioning strategy for backpropagation in detail.

858

- 859 • Case 1, in which we compute the gradient for the weight of the LoRA B projection. We partition  
860 along the output dimension ( $k$ ) for the LoRA B projection matrix to ensure that the gradient computa-  
861 tion correctly associates the  $i$ th LoRA’s slice with the corresponding input and output matrix slices.  
862 Tiling is done along the output dimension, and LoRA ranks  $r_1$  and  $r_2$  remain in each tile.

863 <sup>1</sup>We replicate the input tokens for each LoRA adapter at the beginning of each fine-tuning iteration.

- 864 • Case 2, in which we compute the gradient for the input of the LoRA B projection. We tile over the  
865 sequence dimension and the LoRA rank dimension of the upstream gradient, and reduce over the  
866 input hidden dimension.
- 867 • Case 3, in which we compute the gradient for the weight of the LoRA A projection. We tile over the  
868 sequence dimension of input activations and the output dimension of the upstream gradients, using  
869 LoRA rank as the reduction axis.
- 870 • Case 4, in which we compute the gradient for the input of the LoRA A projection. We tile along  
871 the upstream gradients’ sequence and LoRA rank dimensions and use the concatenated LoRA rank  
872 dimension for reduction.

874 **Kernel performance tuning.** To achieve high kernel performance across different hardware setups,  
875 we tune the ThreadblockShape, WarpShape, and InstructionShape parameters in CUTLASS Thakkar  
876 et al. (2023) to optimize performance. While the optimal settings vary depending on both the  
877 underlying hardware architecture and the GEMM problem dimensions, we simulate workloads using  
878 model dimensions from widely used 3B and 7B models, as well as sequence lengths ranging from  
879 512 to 2048. We set the InstructionShape to (16, 8, 16) to match the tensor core instruction shape on  
880 Ampere GPUs. For WarpShape, we empirically found that (64, 64, 32) yields the best throughput on  
881 the A100, while (16, 64, 32) performs best on the A10 without triggering memory errors. Based on  
882 these warp shapes, we configure ThreadblockShape as (128, 128, 32) on the A100 and (64, 64, 32)  
883 on A10 to ensure compatibility with WarpShape.

## 884 D PROOF OF GREEDY SCHEDULING TAIL EFFECT

887 **Algorithm analysis.** Algorithm 2 performs optimally in a streaming setting with an unlimited number  
888 of jobs, as it consistently selects the job with the highest concurrent LoRA fine-tuning throughput.  
889 However, in our setting with a finite number of jobs, this approach can lead to a tail effect: the final  
890 jobs may not fully utilize all available hardware resources, resulting in suboptimal overall throughput  
891 compared to the optimal solution. We now bound this tail effect.

892 **Theorem D.1** (Bounded Tail Effect with Algo 2). *Let  $J$  be a set of jobs scheduled on  $G$  GPUs. Let  
893  $j \in J$  be the last job that uses  $D$  GPUs. Let  $T_{\text{last}}$  be the fine-tuning time of the last job and  $F$  be  
894 the makespan based on the job planner’s schedule. Then, the approximation ratio (AR) of the job  
895 planner for the makespan optimization problem is upper bounded by:  $AR \leq \frac{F}{F - T_{\text{last}} \frac{G - D}{G}}$ .*

896 See Appendix D for the detailed proof. In practice, using experiment settings from §6, we find that  
897 PLORA produces schedules with AR between 1.05 and 1.14.

900 *Proof.* We start by noting that before starting the last job, all  $G$  GPUs are fully utilized by the  
901 definition of our greedy scheduling algorithm. Moreover, our algorithm offers a monotonicity  
902 condition: if a job using  $x$  GPUs is scheduled, the next job in the optimal ordering requires no more  
903 than  $x$  GPUs. This condition guarantees no bubbles between jobs in the fully loaded batches; the  
904 only underutilization occurs in the final batch.

905 Define the total GPU work as  $W = \sum_{j \in J} x_j t_j$ . Recall that  $t_{\text{last}}$  denotes the processing time of the  
906 last job and the cumulative time of the fully utilized jobs before starting the last job be  $F_{\text{prev}}$ . Let  
907  $F = F_{\text{prev}} + t_{\text{last}}$  be the makespan of the job planner’s schedule, and  $\text{OPT}$  be the makespan of an  
908 optimal schedule with full GPU utilization throughout. Then we can write:

$$910 W = F_{\text{prev}} \cdot G + t_{\text{last}}(G - D),$$

911 and the total makespan of the greedy schedule is

$$913 F = F_{\text{prev}} + t_{\text{last}}.$$

915 An optimal schedule (with full GPU utilization in every batch) must satisfy

$$917 \text{OPT} \geq \frac{W}{G} = F_{\text{prev}} + t_{\text{last}} \frac{G - D}{G}.$$

918  
 919 Table 7: The normalized throughput improvement of packed LoRA kernels over sequential LoRA  
 920 computations. The first number in each cell represents the throughput speedup in the forward pass,  
 921 while the second number represents that in the backward pass.

922	Num. LoRA	3B Attention	3B MLP	7B Attention	7B MLP
923	d = 2048	11008	3584	18944	
924	2	2.00x / 2.01x	1.98x / 1.98x	1.90x / 1.92x	1.99x / 1.99x
925	8	7.98x / 7.96x	7.60x / 7.67x	7.51x / 7.92x	7.77x / 7.80x
926	32	29.0x / 30.0x	26.5x / 26.9x	26.7x / 31.2x	28.4x / 28.7x

927 Thus, we can bound the extra time incurred due to the bubble in the last batch by

$$929 \quad F - \text{OPT} \leq [F_{\text{prev}} + t_{\text{last}}] - \left[ F_{\text{prev}} + t_{\text{last}} \frac{G - D}{G} \right] \quad (21)$$

$$930 \quad = t_{\text{last}} \left( 1 - \frac{G - D}{G} \right) \quad (22)$$

$$931 \quad = t_{\text{last}} \frac{D}{G} \quad (23)$$

932 This result quantifies the tail effect under asynchronous scheduling: the extra time is proportional to  
 933 the fraction of idle GPUs for the last job. And we can obtain our final bound:

$$934 \quad \frac{F}{\text{OPT}} \leq 1 + \frac{t_{\text{last}} \cdot \frac{D}{G}}{F_{\text{prev}} + t_{\text{last}} \cdot \frac{G - D}{G}} \quad (24)$$

935 which can be simplified to

$$936 \quad \frac{F}{\text{OPT}} \leq \frac{F}{F - T_{\text{last}} \cdot \frac{G - D}{G}}.$$

937  $\square$

## 938 E ADDITIONAL EXPERIMENT RESULTS

### 939 E.1 MICROBENCHMARKS

#### 940 E.1.1 PACKED LORA KERNEL PERFORMANCE.

941 We examine the performance of our customized LoRA kernels in various workloads on A100 GPUs.  
 942 Consider a LoRA tensor with a shape  $[r, d]$ , where  $r$  is the LoRA rank and  $d$  is the hidden dimension  
 943 in the base model. We vary both  $r$  and  $d$  to evaluate the computational efficiency of the packed LoRA  
 944 kernel. We first fix  $r = 64$ , set  $d$  to different values based on the hidden dimensions in the Attention  
 945 and MLP layers of QWen-2.5-3B and QWen-2.5-7B, and set the batch size to 1. We pack different  
 946 numbers of LoRA computations into a kernel (ranging from 2 to 32) and compare the forward and  
 947 backward computation performance with a sequential baseline.

948 Table 7 reports the throughput improvement normalized to the performance of the baseline. As we  
 949 increase the number of packed LoRA computations from 2 to 32, our packed LoRA kernels exhibit  
 950 close to linear speedups over the baseline in both forward and backward propagation. This trend  
 951 holds for a wide range of hidden dimensions, from 2048 to 18944, as well as LoRA ranks, from 8 to  
 952 128.

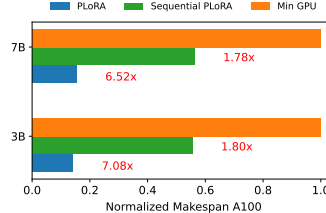
953 In Table 8, we present kernel speed-up as we scale up LoRA forward and backward kernels on A10  
 954 GPUs.

#### 955 E.1.2 SPEEDUP BREAKDOWN.

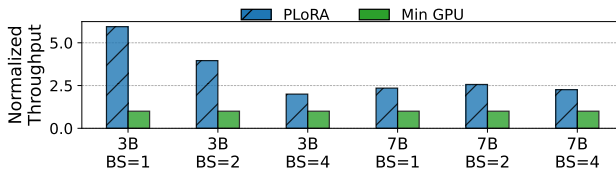
956 PLORA’s performance gains mainly come from two components: optimized GPU kernels for efficient  
 957 packed LoRA computations and near-optimal scheduling for packing LoRA configurations. This

972  
 973 Table 8: In this table, we show the throughput improvement of attention and MLP forward and  
 974 backward LoRA kernels using sequence length 1024 on A10 GPUs as we scale up the number of  
 975 concurrent LoRA adapters. The first number in each cell represents the throughput improvement  
 976 (FLOP/s) of the forward pass, while the second number represents the backward pass.

# LoRA Dim	3B Attention 2048	3B MLP 11008	7B Attention 3584	7B MLP 18944
2	1.98x/1.98x	1.9x/1.86x	1.94x/1.97x	1.98x/1.90x
8	7.65x/7.55x	7.52x/7.42x	7.48x/7.4x	7.44x/7.5x
32	25.95x/26.09x	25.87x/26.14x	27.24x/26.45x	26.78x/26.97x



991 Figure 6: This figure shows the breakdown of PLORA’s speedup on A100 GPUs. Sequential  
 992 PLORA represents the speedup obtained via leveraging PLORA’s Packing Planner, but performs  
 993 vanilla sequential LoRA training without PLORA’s Execution Engine.



1001 Figure 7: This figure shows the LoRA fine-tuning throughput for various models and batch sizes on  
 1002 A10 GPUs normalized to the Min GPU baseline.

1003  
 1004 ablation study breaks down how each component contributes to the overall reduction in makespan.  
 1005 We compare the makespan of LoRA hyperparameter tuning with Min GPU, using PLORA for job  
 1006 planning but executing LoRA sequentially (Sequential PLORA), and PLoRA. The results normalized  
 1007 to Min GPU are shown in Figure 6. We use QWen-2.5-3B and QWen-2.5-7B as base models and use  
 1008 a search space consisting of 120 LoRA configurations. Sequential PLORA reduces the makespan  
 1009 by around 1.8 $\times$  for both models via amortizing the base model computation. The optimized GPU  
 1010 kernels further reduce the makespan by up to 3.93 $\times$ , demonstrating that both components contribute  
 1011 significantly to PLORA’s performance.

## E.2 FINE-TUNING THROUGHPUT ON A10 GPUs

1015 We evaluate PLORA on A10 GPUs using the QWen-2.5-3B and QWen-2.5-7B models, with a LoRA  
 1016 rank of 32. The throughput of LoRA fine-tuning jobs is shown in Figure 7, and the performance is  
 1017 normalized to the Min GPU baseline. PLORA achieves 5.94 $\times$  speedup for 3B and 2.56 $\times$  speedup  
 1018 for 7B. The throughput improvement is lower than that on A100 GPUs, which is expected because  
 1019 A10 GPUs have less GPU memory capacity than A100 GPUs and, therefore, can pack fewer LoRA  
 1020 adapters in LoRA fine-tuning jobs.

1021 We also evaluate PLORA on base models with QLoRA Dettmers et al. (2023), which quantizes the  
 1022 weights of the base model to 4 bits. QLoRA reduces the GPU memory usage of the base model,  
 1023 leaving more memory for LoRA adapters. We enable QLoRA in PLORA and evaluate the performance  
 1024 with QWen-2.5-7B. We use LoRA with a rank of 32 and a batch size of 1 in all LoRA configurations.  
 1025 PLORA achieves 4.72 $\times$  speedup compared to standard QLoRA fine-tuning with a single LoRA. This  
 1026 experiment shows that quantization, an orthogonal approach to boost LoRA fine-tuning efficiency,

1026 can work with PLORA to further improve fine-tuning throughput by packing more LoRA adapters in  
1027 LoRA fine-tuning jobs.  
1028

1029 **F LLM USAGE**  
1030

1031 We used an LLM to polish the writing by correcting grammar in our completed draft. The LLM was  
1032 not used to survey related work or to propose research ideas.  
1033

1034  
1035  
1036  
1037  
1038  
1039  
1040  
1041  
1042  
1043  
1044  
1045  
1046  
1047  
1048  
1049  
1050  
1051  
1052  
1053  
1054  
1055  
1056  
1057  
1058  
1059  
1060  
1061  
1062  
1063  
1064  
1065  
1066  
1067  
1068  
1069  
1070  
1071  
1072  
1073  
1074  
1075  
1076  
1077  
1078  
1079